



LIBRARY
ROYAL AIRCRAFT ESTABLISHMENT
BEDFORD.

MINISTRY OF TECHNOLOGY
AERONAUTICAL RESEARCH COUNCIL
CURRENT PAPERS

On the Equilibrium Piston Technique in Gun Tunnels

By

*L. Davies, J. D. Regan and
K. A. Dolman.*

LONDON: HER MAJESTY'S STATIONERY OFFICE

1968

Price 6s. 6d. net

July, 1967

On the Equilibrium Piston Technique in Gun Tunnels

- By -

L. Davies, J.D. Regan and K.A. Dolman

SUMMARY

The technique whereby the piston is rapidly brought to rest at the end of the gun tunnel barrel, and the pressure peak which results is equal in magnitude to the final equilibrium pressure, is called the equilibrium piston technique. This technique was first demonstrated by East and Pennelegion. Details of the various formulae available for calculating the peak pressures are given, and from Stalker's formula an equation is derived which relates the equilibrium piston mass to the dimensions and initial conditions within the gun tunnel. Experiments performed in the NPL 2 in. gun tunnel using 20 and 25 gm pistons are described and shown to agree with theory. In all cases nitrogen was used as driver and test gas.

List of Contents

	<u>Page</u>
1. Introduction	3
2. Theory	4
2.1 Simple gun-tunnel behaviour	4
2.2 Estimation of peak pressure	5
2.3 Reduction of peak pressure	6
2.4 Estimation of equilibrium pressure	10
2.5 Estimation of equilibrium temperature	11
2.6 Effect of diaphragm area ratio on performance	12
2.7 Estimation of running time	13
3. Experiment	15
3.1 Description of gun-tunnel	15
3.2 Tunnel performance capability	16
3.3 Some preliminary experimental results	16
4. Conclusions	16

List/

List of Symbols

a	speed of sound
a*	speed of sound in nozzle throat
a_{ij}	a_i/a_j
A	cross-sectional area
A_{ij}	A_i/A_j
B	constant in Eqn. (14)
B'	constant in Eqn. (33)
C	constant in Eqn. (34)
D	constant in Eqn. (35)
F	frictional force between piston and barrel walls
g	acceleration due to gravity, except in Section 2.7 where it is defined as in Eqn. (23)
k_1	factor which arises from the unsteady expansion and recompression of the gas behind the piston
L	length
m	mass
m_e	mass of equilibrium piston
\bar{m}_e	non-dimensionalised piston mass, $m_e/p_1 A_1$
M	Mach number
M_R	Mach number of first reflected shock from end wall
p	pressure
\hat{p}	peak pressure
P_{ij}	p_i/p_j
r	radius
r^*	radius of nozzle throat
R	universal gas constant
t	time
t_*	time taken for reservoir gas to pass through nozzle throat
T	temperature

u	velocity
U_2	maximum piston velocity, assumed equal to the contact surface velocity in shock tube flow
U_{ij}	u_i/a_j , except $U_{21} = U_2/a_1$
x	distance along gun tunnel channel
x_1	distance from the end wall of the point of interaction of the first reflected shock with the piston
x_2	distance of the piston, from the end wall, in its equilibrium condition, see Fig. 1
z	x/x_2
α_i	$(\gamma_i + 1)/(\gamma_i - 1)$
β_i	$(\gamma_i - 1)/2\gamma_i$
γ	ratio of specific heats, c_p/c_v
ψ	defined in Eqn. (14)
ϕ	defined in Eqn. (14)
λ	constant in Eqn. (32)
ω	frequency of piston oscillation

Subscripts

- 1,2,3,4, etc. refer to the regions of flow shown in Fig. 1
- e refers to the equilibrium condition

1. Introduction

The main attraction of the gun tunnel, as compared with the conventional shock tunnel, is its promise of long running times. The shock tunnel, operating at its so called 'tailoring' condition, has a testing time typically of the order of 5 milliseconds. Consequently measuring techniques have to respond within about a millisecond to changes which occur in the flow. A representative gun-tunnel running time is about 50 milliseconds, greater by a factor of 10 compared with the shock tunnel. The instrument response-time problem is therefore less acute, the range of available techniques wider, and the task potential of the tunnel is greater.

As a result of considerations of gain in running time, it was decided to convert the NPL 2 in. shock tunnel into a gun tunnel. As the test gas in a gun tunnel is compressed and heated (non-isentropically) by a light, fast-moving piston, first consideration is the optimum piston weight. Although various

aspects/

aspects of the influence of piston weight on gun-tunnel performance have been studied, it is not possible to decide from the existing literature what piston weight is required for various conditions. Therefore the main study, reported in this paper is of the relation between piston weight and tunnel conditions.

The most promising line of attack appeared to be that used by East and Pennelegion¹. In this approach the conditions are obtained under which the piston is brought rapidly to rest at the end of the channel (Fig. 1), in a 'dead-beat' action. This results in the smallest amount of fluctuation in the reservoir pressure, and avoids very high pressure peaks caused by piston overshoot. These points are discussed in detail in Section 2. From this study a simple analytical model emerged which describes the relationship between piston weight, initial tunnel conditions and tunnel geometry.

The problem outlined above is described together with a discussion of the reservoir conditions in a gun tunnel, and the factors which influence them. Some experimental results from the NPL 2 in. gun tunnel are also presented.

2. Theory

2.1 Simple gun-tunnel behaviour

The gun-tunnel differs from the shock tunnel only in the use of a light piston to compress the test gas. The piston is initially placed against the downstream side of the main diaphragm, and when the diaphragm bursts the piston is accelerated down the channel, causing the gas ahead of it to be heated and compressed, partly by a shock wave travelling ahead of the piston and partly by means of an adiabatic compression of the gas. When the piston nears the end of the channel this shock wave reflects from the end plate and interacts with the piston causing it to decelerate. There are several shock reflections between the piston and the end wall, and the gas in this volume is compressed non-isentropically to some final temperature and pressure which depend on the initial conditions. The piston path during this process is shown in Fig. 1. The available testing time is then determined by the time it takes for the gas between the piston and the end wall to pass completely through the nozzle.

In elementary gun-tunnel theory it is usual to assume that the piston quickly reaches the velocity of the contact surface in a simple shock tunnel. Shock-tunnel theory is therefore applicable and this makes the estimation of gun-tunnel performance much easier. This assumption is implicit in the theory described in this paper. Further assumptions made in computing the piston motion are that the shock wave ahead of the piston forms immediately but may vary in strength, that the gas between the piston and the shock has uniform thermodynamic properties throughout, that the wave system between the piston and high pressure gas is simple, that the friction between the piston and the walls of the tube does not vary with piston velocity, and that the gas may be assumed to be perfect².

The equation of motion of the piston is then given by East² as:

$$\frac{p_3 - p_2}{p_4} = \frac{du}{dt} \cdot \frac{p_4 \cdot A \cdot g}{a_4^2 \cdot m} + \frac{F}{A \cdot p_4}$$

The pressures p_2 and p_3 in either side of the piston are calculated from the equations

$$p_3/p_4/$$

$$p_3/p_4 = \left[\left(\frac{\gamma_4 + 1}{2} \right)^{\frac{1}{2}} - \frac{\gamma_4 - 1}{2} - \frac{u_2}{a_4} \right] \frac{2\gamma_4}{\gamma_4 - 1}$$

$$p_2 = p_1 \left[\frac{\gamma_1}{2} U_{21} \left\{ U_{21} \frac{\gamma_1 + 1}{2} + \left(U_{21}^2 \left(\frac{\gamma_1 + 1}{2} \right)^2 + 4 \right)^{\frac{1}{2}} + 1 \right\} \right].$$

The equation of motion of the piston is then given as

$$f \left(U_{21}, \gamma_4, \gamma_0 \right) - \frac{F}{A \cdot P_4} = \Lambda \frac{du}{dt}, \text{ where } \Lambda = \frac{p_4 \cdot A \cdot g}{a_4^2 \cdot m}.$$

This may be solved numerically to calculate the piston trajectory.

A more refined approximation for the piston motion is given by Stalker³.

The parameter $\left(\frac{p_4 \cdot A \cdot g}{a_4^2 \cdot m} \right)$ is most important in the analysis of the piston motion

since it affects the accelerating phase and the maximum velocity the piston may attain. A detailed account of the piston motion may be obtained from Refs. 2 and 3.

By analogy with shock tunnel flows, the initial shock formed ahead of the piston will be called the primary shock. This shock reflects from the end wall and interacts with the piston. The subsequent shock reflections, first from the piston then from the end wall, cause a very high peak in pressure in the gas at the end wall, and hence in the test-flow stagnation pressure. These peaks can reach three and four times the original driver gas pressure. Several pressure peaks of lesser magnitude subsequently occur due to further shock reflections between the piston and the end wall, and during this time the piston can execute several oscillations about some mean position a short distance from the end wall. These points are illustrated in Fig. 1.

Some methods of estimating the magnitude of these peak pressures are given in the following section.

2.2 Estimation of peak pressure

Equations relating the peak pressure to the initial tunnel conditions have been derived by Stalker³ and by Edney⁴, and these will be discussed below.

Stalker found that it is possible to neglect entropy changes after the first shock reflection from the piston, and also that to a first approximation the expansion waves which occur as the piston decelerates are fairly weak and can be neglected. It is therefore possible to consider that at any instant the pressure between the shock and each of the two adjacent boundaries (end wall and piston) is constant. Equating the energy lost by the piston, plus the work done on the piston by the driver gas, with the energy gained by the compressed gas, Stalker obtained the following equation for peak pressure

$$\hat{p} = p_5 \left[1 + (\gamma - 1) P_{35} + \frac{\gamma - 1}{2} \cdot \frac{m U_2^2}{p_5 x_1 A} \right]^{\frac{\gamma}{\gamma - 1}} \quad \dots(1)$$

where

$$x_1 = \frac{M_{R1}}{M_1} \cdot L \cdot \frac{(M_1 - U_{21})}{(M_{R1} + U_{21})} = \begin{array}{l} \text{distance from end wall} \\ \text{of point of interaction of} \\ \text{1st reflected shock with piston.} \end{array}$$

Edney⁴ has proposed a similar formula for estimating peak pressure based on much cruder approximations. This formula has the form

$$\hat{p} = p_5 \left[1 + \frac{(\gamma_1 - 1)}{2} \cdot \frac{m U^2}{p_1 L A} \right]^{\frac{\gamma}{\gamma - 1}} \quad \dots(2)$$

Eqns. (1) and (2) are approximate and are intended to give only an order of magnitude for the peak pressure. Values obtained using these equations are shown in Fig. 3 where the peak pressures predicted by Eqn. (1) are higher than those from Eqn. (2).

Stalker found that Eqn. (1) gave a reasonably good representation of the peak pressure values for various p_1 , and so Eqn. (1) is to be favoured for such estimates.

2.3 Reduction in peak pressure

Reduction of the peak pressure which occurs at the start of a gun-tunnel run is the subject of a paper by East and Pennelegion¹. In this paper a 'dead-beat' piston mode of operation is described where the piston is brought to rest by the first reflected shock from the end wall. The peak pressure is then equal to the final equilibrium pressure, and the technique is therefore called the equilibrium-piston technique.

From momentum considerations East and Pennelegion found that the equilibrium piston mass in the non-dimensional form

$$\bar{m}_e = \frac{m_e}{p_1 A} \quad \dots(3)$$

was a function of $\left(\frac{P_{e4} \cdot P_{41}}{U} \right)$, and concluded that the dominant term was P_{41} ; as P_{41} increased so did \bar{m}_e . No equation for equilibrium piston mass was given from which the piston masses could be calculated for specified initial conditions. It was therefore decided that the equations for peak pressure given by Stalker and Edney might be used to do this.

Stalker's equation for peak pressure, quoted above, is

$$\hat{p} = p_5 \left[1 + (\gamma - 1) P_{35} + \frac{(\gamma - 1) m U_2^2}{2 p_5 x_1 A} \right]^{\frac{\gamma}{\gamma - 1}} \quad \dots$$

Assuming/

Assuming that for equilibrium $\hat{p} = p_e$, it follows that

$$\frac{\hat{p}}{p_e} \cdot \frac{p_e}{p_4} \cdot \frac{p_4}{p_1} = P_{51} \left[1 + (\gamma - 1) P_{35} + \frac{(\gamma - 1) m U_2^2}{2 p_5 x_1 A} \right]^{\frac{\gamma}{\gamma - 1}}, \quad \dots(4)$$

and hence at equilibrium

$$P_{e4} \cdot P_{41} = P_{51} \left[1 + (\gamma - 1) P_{35} + \frac{(\gamma - 1) m_e U_2^2}{2 p_5 x_1 A} \right]^{\frac{\gamma}{\gamma - 1}} \dots(5)$$

The non-dimensional piston mass is defined as $\bar{m}_e = \frac{m_e}{p_1 A}$ and so from Eqn. (5) we have

$$\bar{m}_e = \frac{2x_1}{(\gamma - 1)} \cdot \frac{P_{51}}{U_2^2} \left[\left(\frac{P_{e4} P_{41}}{P_{51}} \right)^{\frac{\gamma - 1}{\gamma}} - (1 + (\gamma - 1) P_{35}) \right] \dots(6)$$

Similarly, the equation for peak pressure given by Edney is

$$\hat{p} = p_5 \left[1 + \frac{(\gamma - 1) m U_2^2}{2 p_1 LA} \right]^{\frac{\gamma}{\gamma - 1}}$$

and proceeding as before we have for the non-dimensional piston mass at equilibrium

$$(\bar{m}_e)^* = \frac{2L}{(\gamma - 1)} \cdot \frac{1}{U_2^2} \left[\left(\frac{P_{e4} P_{41}}{P_{51}} \right)^{\frac{\gamma - 1}{\gamma}} - 1 \right] \dots(7)$$

Values of \bar{m}_e for various P_{41} were calculated using Eqn. (6) and (7). It was found that Eqn. (6) gave far better agreement with experiment, using data given by East and Pennelegion and that obtained in the NPL gun tunnel by the present authors, than values obtained from Eq. (7) (see Fig. 4). Eqn. (6) was therefore adopted for further equilibrium piston calculations.

From calculations of equilibrium piston mass versus initial conditions in the gun tunnel for nitrogen as driver and driven gases, the following observations can be made:

- (a) The equilibrium piston mass \bar{m}_e increases with increasing P_{41} (see Fig. 4).

(b)/

- (b) When a piston mass is chosen and fixed, the theoretical curve of p_4 versus p_1 , or P_{41} , for equilibrium conditions has a minimum with respect to the p_4 axis. This means that for a fixed piston weight there exists a minimum value of p_4 below which equilibrium conditions cannot be obtained for any P_{41} . This is seen in Fig. 10, where the minimum p_4 for a 20 gm piston is about 2000 psi in a 2 in. gun-tunnel.
- (c) For a given driver pressure above this minimum, there exists two discrete values of P_{41} at which one piston mass will give equilibrium conditions. The range of p_4 values for which this occurs is limited and depends on the piston mass.
- (d) In gun-tunnels the distance between the piston and the shock which travels ahead of it down the tube, is found to be less than that predicted from simple theory. As a result the value of x_1 will be less. Using a value of x_1 which is 0.65 times less than the simple theory value, a figure which has been quoted in the literature, then it is seen from Fig. 4 that the curve agrees more closely with experiment. Clearly x_1 must be determined experimentally for each particular facility, but an improvement in \bar{m}_e prediction should result from using the actual value of x_1 .

Alternative solutions for \bar{m}_e

In the preceding analysis a relationship for the equilibrium-piston mass was obtained from the equation for peak pressure. An alternative equilibrium-piston analysis has been carried out by Smith⁸ who considered the motion of the piston when it had almost reached its final position near the end of the barrel. The motion of the piston as a result of a small perturbation was then investigated. From the equation of piston motion the conditions required for critical damping were found and an equilibrium-piston mass obtained.

The equation for piston motion derived by Smith, is

$$m \frac{d^2x}{dt^2} + \frac{A k_1 p_4 \gamma_4}{a_3} \cdot \frac{dx}{dt} + \frac{A k_1 p_4 \gamma_1}{x_2} \cdot x = 0 \quad \dots(8)$$

where x_2 is the final position of the piston at the end of the channel when the quasi-steady reservoir conditions exist, and k_1 is a factor which arises from the unsteady expansion and recompression of the gas behind the piston during its motion down the barrel.

The equation of motion has a solution of the form

$$x = e^{(-t/\tau)} \sin \omega t \quad \dots(9)$$

where
$$\tau = \frac{2 a_3 m}{A k_1 p_4 \gamma_1}, \quad \omega^2 = \frac{A k_1 p_4 \gamma_1}{m x_2} - \frac{A^2 k_1 p_4^3 \gamma_4^2}{4 a_3^3 m^2} .$$

For critical damping $\omega^2 = 0$

which gives
$$m_e = \frac{A k_1 p_4 \gamma_4^2 x_2}{4 a_3^2 \gamma_1} \dots(10)$$

or
$$m_e = \frac{A p_e x_2}{4 \gamma_1} \left(\frac{\gamma_4}{a_3} \right)^2 \dots(11)$$

An analysis of the motion of the piston near the end of the barrel has also been made by Stalker³ from which a relationship of m_e can be obtained. The equation of motion in this case is

$$\frac{m x_2}{A p_e} \frac{d^2 z}{dt^2} + \frac{\gamma_4 x_2}{a_e} \cdot \frac{dz}{dt} = z - \gamma - 1 \dots(12)$$

here $z = x/x_2$. As regards damping Stalker considers the solution near $z = 1$ is the appropriate case where the velocities are highest and the driving term is lowest. The equation of motion is thus linearized into a form suitable for $|z - 1| \ll 1$. The equation is then

$$\frac{m x_2}{A p_e} \frac{d^2 z}{dt^2} + \frac{\gamma_4 x_2}{a_e} \frac{dz}{dt} + \gamma (z - 1) = 0 \dots(13)$$

This has the solution

$$z - 1 = B e^{-\psi t} \sin(\omega t + \phi) \dots(14)$$

where

$$\psi = \frac{1}{2} p_e \gamma_4 A/m a_e, \omega = \frac{1}{2} \left(\frac{A p_e \gamma_4}{m a_e} \right) \left\{ \frac{4 m \gamma}{A p_e x_2} \left(\frac{a_e}{\gamma_4} \right)^2 - 1 \right\}^{\frac{1}{2}}$$

and ϕ and B are constants.

Here again the critical damping case corresponds to $\omega^2 = 0$ and this requires that

$$\frac{4 m \gamma}{A p_e x_2} \left(\frac{a_e}{\gamma_4} \right)^2 - 1 = 0.$$

The equilibrium piston weight is therefore

$$m_e = \frac{A p_e x_2}{4 \gamma_1} \cdot \left(\frac{\gamma_4}{a_e} \right)^2 \dots(15)$$

This equation closely resembles Eqn. (11) obtained by Smith. The only difference is in the sound speed used. This is critical however and from plots of \bar{m}_e versus P_{41} in Fig. 4 it is seen that whereas the Smith solution is of the same order of magnitude as values obtained from the peak pressure analysis for the higher P_{41} values, the values obtained from Eqn. (15) above are about a factor 10 different over most of the P_{41} range as compared with values obtained using Eqn. (6). Clearly the 'peak pressure analysis' values of \bar{m}_e are in best agreement with the experimental trend and will be used throughout the rest of this paper.

2.4 Estimation of equilibrium pressure

It is assumed in this section that the piston is brought to rest after interaction with the first reflected shock from the end wall. As the piston slows down the compression waves facing upstream, produced by the piston, coalesce into a shock, which propagates back towards the main diaphragm. The pressure ratio across the wave is P_{e3} and the flow velocity behind the piston is u_e where suffix 'e' is used to denote the equilibrium condition, (see Fig. 1). Since the piston comes to rest, the flow velocity at the piston is zero. Therefore in fixed co-ordinates appropriate to region (3), $u_3 = u_e$. Defining $\frac{u_3}{a_3} = M_3$ the relationship for P_{e3} , in terms of M_3 and γ_4 , is

$$P_{e3} = \frac{1}{2} \left[\left\{ 2 + \frac{\gamma_3(\gamma_3+1)}{2} M_3^2 \right\} + \left\{ \gamma_3(\gamma_3+1) M_3^2 \left(1 + \frac{\gamma_3(\gamma_3+1)}{4} M_3^2 \right) - 2 \gamma_3 M_3^2 (\gamma_3-1) \right\}^{\frac{1}{2}} \right]. \quad \dots(16)$$

If it is assumed that after rupture of the main diaphragm the piston very quickly reaches its asymptotic velocity, then as for simple shock-tube flow $p_2 = p_3$ and so M_3 may be calculated from the equation

$$M_3 = \frac{1}{\gamma_4 \beta_{44}} \left[(P_{14} \cdot P_{21})^{-\beta_{44}} - 1 \right] \quad \dots(17)$$

where $\beta_{44} = (\gamma_4 - 1)/2\gamma_4$.

Now $P_{34} = P_{14} P_{31}$ and so

$$P_{e4} = P_{e3} \cdot P_{34} = P_{e3} \left[1 - \frac{(\gamma_4 - 1)}{(\gamma_4 + 1)} \frac{(M_1^2 - 1)}{a_{41} M_1} \right]^{\frac{1}{\beta_{44}}}, \quad \dots(18)$$

where/

where M_1 is the Mach number of the shock produced ahead of the piston as it first moves down the channel. Values of M_1 in terms of piston velocity are readily obtained from shock flow tables, for example from Bernstein's⁵ tables for nitrogen, or oxygen, as test gas.

Values of p_{e4} and P_{41} are given in Table 1 for nitrogen as driver and driven gases and for $A_{41} = 1$.

TABLE I

P_{41}	P_{e4}	P_{41}	P_{e4}
9.76	0.995	109	0.741
18.4	0.955	194	0.656
33.7	0.886	349	0.564
60.8	0.827		

2.5 Estimation of equilibrium temperature

In Section 2.3, it was assumed that entropy changes, which occurred after the first shock reflected from the end wall, could be neglected. This led to a considerable simplification in the estimation of equilibrium pressure conditions. The same simplification can be employed to estimate the equilibrium temperature.

If the temperature behind the first reflected shock be denoted by T_5 , and the equilibrium temperature by T_e , then the ratio of T_5 to T_e is given by

$$\frac{T_5}{T_e} = \left(\frac{P_{51}}{P_{e4} \cdot P_{41}} \right)^{\frac{\gamma_1 - 1}{\gamma_1}} \quad \dots(19)$$

and therefore

$$T_e = T_5 \left(\frac{P_{51}}{P_{e4} \cdot P_{41}} \right)^{\frac{1 - \gamma_1}{\gamma_1}} \quad \dots(20)$$

The ratio T_e/T_1 is thus

$$\frac{T_e}{T_1} = \frac{T_5}{T_2} \cdot \frac{T_2}{T_1} \left(\frac{P_{51}}{P_{e4} \cdot P_{41}} \right)^{\frac{1 - \gamma_1}{\gamma_1}} \quad \dots(21)$$

where/

where

$$\frac{T_5}{T_2} = \frac{P_{51} \cdot P_{12} (\alpha_1 + P_{51} \cdot P_{12})}{1 + \alpha_1 P_{51} P_{12}}$$

and

$$\frac{T_2}{T_1} = \frac{[2 \gamma_1 M_1^2 - (\gamma_1 - 1)] [(\gamma_1 - 1) M_1^2 + 2]}{(\gamma_1 + 1)^2 M_1^2}$$

Values of T_e , calculated using the above equations, can only be expected to be approximate, and a comparison between these theoretical values and actual values is given in Fig. 5. In this figure a curve estimated by NRC obtained from Ref. 6 is given, along with experimental data obtained by Stollery⁷, and curves prepared using Eqn. (20). The curves of temperature behind the first reflected shock and of the isentropic compression of the test gas to p_e are also given and are seen to lie below the experimental data. For the lower values of P_{41} the temperature T_e obtained by experiment lies between the $A_{41} > 1$ curves obtained from Eqn. (20), but the $A_{41} = 1$ curve agrees best with experiment for $P_{41} > 100$.

2.6 Effect of diaphragm area ratio on performance

It has been shown by Alpher and White⁶ that shock tubes which have a larger driver cross-sectional area than channel cross-sectional area can produce higher primary shock Mach numbers than shock tubes of constant cross section, for the same P_{41} value. East² has shown that the same advantage is gained in gun tunnel operation.

The equations used for obtaining an estimate of the primary shock Mach number to be expected with an area change at the main diaphragm have been derived by Alpher and White (loc.cit.). If it is assumed that the piston reaches its asymptotic velocity very quickly, then the relation between piston velocity, normalised with respect to the initial speed of sound in the test gas, in terms of the ratio P_{41} is

$$P_{41} = \frac{P_{21}}{g} \cdot \left[1 - \frac{U_{21}}{a_{41}} \cdot \frac{\gamma_4 - 1}{2} \cdot g^{-\beta_4} \right]^{-\frac{1}{\beta_4}} \quad \dots(22)$$

where

$$g = \left\{ \left[\frac{2 + (\gamma_4 - 1) M_u^2}{2 + (\gamma_4 - 1) M_{st}^2} \right]^{\frac{1}{2}} \cdot \left[\frac{2 + (\gamma_4 - 1) M_{st}^2}{2 + (\gamma_4 - 1) M_u^2} \right] \right\}^{\frac{1}{\beta_4}} \quad \dots(23)$$

and/

and the area change determines the Mach numbers M_u and M_{st} through the equation

$$A_{41} = \frac{A_4}{A_1} = \frac{M_{st}}{M_u} \left[\frac{2 + (\gamma_4 - 1) M_u^2}{2 + (\gamma_4 + 1) M_{st}^2} \right]^{\frac{\alpha_4}{2}} \dots (24)$$

The Mach numbers M_u and M_{st} are intermediate flow Mach numbers during the unsteady-steady expansion of the driver gas. M_u is related to the unsteady and M_{st} to the steady expansion.

For a constant cross-section in the tunnel ($A_{41} = 1$)

$$P_{41} = P_{21} \left[1 - \frac{U_{21}}{a_{41}} \cdot \frac{\gamma_4 - 1}{2} \right]^{-\frac{1}{\beta_4}} \dots (25)$$

Comparing this equation with Eqn. (22), it is clear that a tunnel with area ratio $A_{41} \neq 1$, pressure ratio P_{41} , and sound speed ratio a_{41} will produce a primary shock Mach number equal to that produced by a tunnel with $A_{41} = 1$, diaphragm pressure ratio $P_{41} g$, sound speed ratio $a_{41} (g)^{\beta_4}$, with the same γ_4, γ_1 .

The effect on equilibrium piston operation is that when values of \bar{m}_e are calculated for $A_{41} > 1$ it is found that, at the same value of P_{41} , (\bar{m}_e) for $A_{41} = 1$ is greater than (\bar{m}_e) for $A_{41} > 1$. If it is argued that for $A_{41} > 1$ a lower P_{41} is required to give the same piston velocity than for $A_{41} = 1$, it is immediately clear from Fig. 4 that, using Eqn. (7), the value of \bar{m}_e obtained for $A_{41} > 1$ will be even lower than for the $A_{41} = 1$ case. This is because \bar{m}_e decreases as P_{41} decreases.

Therefore the piston weights required for equilibrium operation for a given channel diameter and p_1 will be greater for a tunnel where $A_{41} = 1$ than for one with $A_{41} > 1$. For small diameter tunnels (e.g., the NPL 2 in. gun-tunnel), this can often mean the difference between having a reasonable weight piston, i.e., 20 or 30 gms, and having to produce very light pistons (about 5 or 6 gms.) needed if $A_{41} > 1$.

On piston weight considerations the suggestion is therefore that the constant driver-channel cross-section tunnel is preferred to the $A_{41} > 1$ geometry.

2.7 Estimation of running time

An estimation of running time in the gun-tunnel may be obtained by calculating the initial mass of gas in the channel and considering the time it takes for this mass at the stagnation temperature and pressure, T_e and P_e , to pass through the nozzle. Here piston friction is ignored, and p_e is assumed to remain constant during the testing time.

The/

The initial mass of gas in the channel is given by

$$\text{Mass} = \rho_1 \pi r^2 L = m_i \quad \dots(26)$$

This mass is raised to a pressure p_e and temperature T_e which depend on the initial diaphragm pressure ratio P_{41} . The rate of mass flow through the nozzle is given by

$$\frac{dm}{dt} = \dot{m} = \rho^* a^* A_T = \rho^* a^* \pi r^{*2} \quad \dots(27)$$

The time taken for the reservoir gas to pass completely through the nozzle is

$$t_* = \frac{m_i}{\dot{m}} = \frac{\rho_1 \pi r^2 L}{\rho^* a^* \pi r^{*2}} \quad \dots(28)$$

The so-called critical ratios for the flow of a perfect gas through a nozzle are

$$\frac{p^*}{p} = \left(\frac{2}{\gamma+1} \right)^{\frac{\gamma}{\gamma+1}}, \quad \frac{\rho^*}{\rho} = \left(\frac{2}{\gamma+1} \right)^{\frac{1}{\gamma+1}}, \quad \frac{T^*}{T} = \left(\frac{2}{\gamma+1} \right) \quad \dots(29)$$

Using these relationships and the following expressions

$$a = \sqrt{\gamma RT} = \sqrt{\frac{\gamma p}{\rho}}, \quad \frac{p_1}{p^*} = \frac{p_1}{p_4} \cdot \frac{p_4}{p_e} \cdot \frac{p_e^*}{p^*} \quad \dots(30)$$

Then the time taken for the gas to flow completely through the nozzle is

$$t_* = \frac{L}{P_{41} P_{e4} a_1} \cdot \left(\frac{T_e}{T_1} \right)^{\frac{1}{2}} \cdot \left(\frac{r}{r^*} \right)^2 \cdot \left(\frac{2}{\gamma+1} \right)^{-\frac{\alpha}{2}} \quad \dots(31)$$

If the test gas is nitrogen and if the specific heat ratio is assumed to remain constant at 1.4, then for a given tube the running time is

$$t_* = \frac{\lambda T_e^{\frac{1}{2}}}{P_{e4} P_{41} r^{*2}} \quad \dots(32)$$

where

$$\lambda = \frac{L}{a_1} \cdot \frac{r^2}{T_1^{\frac{1}{2}}} \cdot \left(\frac{2}{\gamma+1} \right)^{\frac{\alpha}{2}} = \text{const.}$$

For fixed throat radius this further reduces to

$$t_* = \frac{B^2 T_e^{\frac{1}{2}}}{P_{e4} P_{41}} \dots (33)$$

Over the range $P_{41} < 100$ for a rough estimate it may be assumed that P_{e4} is constant at a value 0.85 for $A_{41} = 1$ and the running time is obtained using the equation

$$t_* = \frac{C.T_e^{\frac{1}{2}}}{P_{41}} \dots (34)$$

Finally if the driver pressure remains constant then the relation is very simply

$$t_* = D \cdot T_e^{\frac{1}{2}} \cdot P_1 \dots (35)$$

From the foregoing relationships it is easy to determine the most important factors controlling the running time of the gun-tunnel. The running time is directly dependent on the square root of the reservoir temperature; on the reciprocal of the reservoir to driver pressure ratio; and on the reciprocal of the initial diaphragm pressure ratio. If the driver pressure is a constant and it is assumed that $P_{e4} = 0.85$ then from Eqn. (35) it is seen that the running time depends only on the square root of the reservoir temperature and the initial channel pressure.

Plots of running time versus P_{41} are given in Fig. 6, and some experimental results from the NPL gun-tunnel are included showing the good agreement between theory and experiment. The two curves relate to the different throat areas of the working section nozzle.

3. Experiments

3.1 Description of tunnel

The NPL gun-tunnel has a 12 ft long, 2 in. i.d. barrel, (see Fig. 2). The driver chamber has the same internal diameter as the barrel and is 7 ft long. At the end of the driver chamber a perforated plate joins the driver internally to a 3 ft long, 4 in. i.d. reservoir. The use of such a section is known as the driver-reservoir technique, and a detailed description of its principles and operation is given in Ref. 9. At the end of the barrel, throats of $\frac{1}{4}$ or $\frac{1}{2}$ in. diameter can be used to connect the barrel to a 8 in. i.d. working section through a conical 10° half-angle nozzle. The Mach number range in the working section is $8.6 \leq M_{\infty} \leq 11.6$, and it is proposed to extend the lower end of this range to $M_{\infty} = 6$, by means of a contoured nozzle. The test gas is nitrogen, and nitrogen is also used as driver gas at pressures up to 5000 psi. The tunnel is designed to operate at driver pressures up to 10 000 psi, and it is hoped to achieve this value in the near future.

3.2 Tunnel performance

It is assumed that only equilibrium piston operation of the tunnel is contemplated for future tests, and using the above data the curves shown in Figs. 7,8,9 have been derived. Static pressures and temperatures in the working section are shown in Fig. 7 for various P_{41} values and free stream Mach numbers for a 25 gm piston. The stagnation temperatures for these various conditions may be obtained from Fig. 5. It is clear that such plots define the limits within which the gun-tunnel can operate, and an important boundary, i.e., the curve which denotes the occurrence of nitrogen liquifaction in the working section, provides one of these.

The test Reynolds number per inch for the 25 gm piston curve is shown in Fig. 9. It is seen that Reynolds numbers in excess of 10^6 per inch are readily available at the lower Mach numbers. A useful formula (suggested to the authors by S.C. Metcalf) which provides a close approximation to the Reynolds number obtained by more detailed calculations is

$$\text{Re/inch/psi} = \frac{8.4 \times 10^6 \times M_{\infty} (T_{\infty} + 117)}{T_{\infty}^2} \dots(36)$$

The pressure referred to here is the static pressure in the working section. This equation is for nitrogen as working gas, and includes Sutherlands formula for the viscosity-temperature relationship. Some curves obtained using this formula are shown in Fig. 9. To convert this into Re/inch, it is therefore only necessary to multiply the values along the abscissa by the static pressure in psi in the working section.

3.3 Some experimental results

Experiments to determine the tunnel characteristics using 20 and 25 gm pistons have been carried out and the results obtained have been compared with the theory in Section 2.3. The experimental values of \bar{m}_e are compared with theory in Fig. 4. In Fig. 10 the experimental and theoretical values for the variation of piston weight with p_4 for various p_1 are shown. From these data it is seen that a close estimate of equilibrium piston weight can be obtained from the theory given above.

The achievement of equilibrium conditions is determined from measurements of reservoir pressure. When the value of \hat{p}/p_e lies in the range $1 \leq p/p_e \leq 1.1$ it is considered that equilibrium conditions have been obtained. Some pressure records obtained in the NPL gun-tunnel are shown in Fig. 11. The peak and equilibrium pressures obtained from the stagnation pressure record are labelled. The pitot pressure in the working section is also shown. The off-design condition is demonstrated in Fig. 11(c) where a 20 gm piston is used at 1000 psi (below the minimum p_4 for this piston).

Conclusions

The following conclusions are drawn from this study:

- (1) In order to reduce the high peak pressures which are obtained in the reservoir of gun tunnels as the piston comes to rest, and to attain steady reservoir conditions quickly it is necessary to use the equilibrium-piston technique.

(2)/

- (2) Comparison between theory and experiment shows that a close estimate of the piston weight required for equilibrium operation for prescribed conditions can be obtained using the analysis described in Section 2.3.
- (3) From this analysis it is found that the non-dimensional piston mass, \bar{M}_e , increases as $P_{4,1}$ increases. For fixed initial pressure the equilibrium piston weight increases as p_4 increases, for fixed driver pressure there are two values of p_1 at which one piston weight will give equilibrium conditions, and there exists a minimum driver pressure below which equilibrium conditions will not be obtained for a prescribed piston weight.
- (4) Once a piston weight has been decided upon for a particular facility, then the range of test conditions which can be achieved in the working section are closely defined.
- (5) From piston-weight consideration the $A_{4,1} = 1$ geometry is preferred to $A_{4,1} > 1$ for gun-tunnel operation.

References/

References

<u>No.</u>	<u>Author(s)</u>	<u>Title, etc.</u>
1	R.A. East and L. Pennelegion	The equilibrium piston technique for gun-tunnel operation. A.R.C. C.P. 607 April, 1961.
2	R.A. East	The performance and operation of the University of Southampton hypersonic gun tunnel. AASU Report No. 135, August, 1960.
3	R.J. Stalker	Rebound of a high speed piston by gas compression in a closed tube. NRC Canada Mech. Eng. Rep. MT-42. March, 1961.
4	B. Edney	Factors limiting the maximum stagnation temperatures in a gun tunnel. ICAS Paper No. 66-23, 5th Int. Council of Aeron. Sci. September, 1966.
5	L. Bernstein	Tabulated solutions of the equilibrium gas properties behind the incident and reflected normal shock wave in a shock tube. I. Nitrogen. II. Oxygen. A.R.C. C.P. No. 626, April, 1961.
6	R.A. Alpher and E.R. White	Flow in shock tubes with area change at the diaphragm section. J. Fluid Mechanics, Vol. 3, Part 5, p.457. Feb., 1958.
7	J.L. Stollery	Stagnation temperature measurements in a hypersonic gun tunnel using the sodium line reversal method. A.R.C.22 854 - Hyp.187. 1961.
8	F. Smith	· ARDE Internal Report (unpublished).
9	L. Davies and K.A. Dolman	On the driver-reservoir technique in shock and gun tunnels. NPL Aero Report 1226. A.R.C.28 957. April, 1967.
10	R. N. Cox	Recent hyperballistics research at ARDE Proc. 11th Symposium of the Colston Res. Soc. 1959.

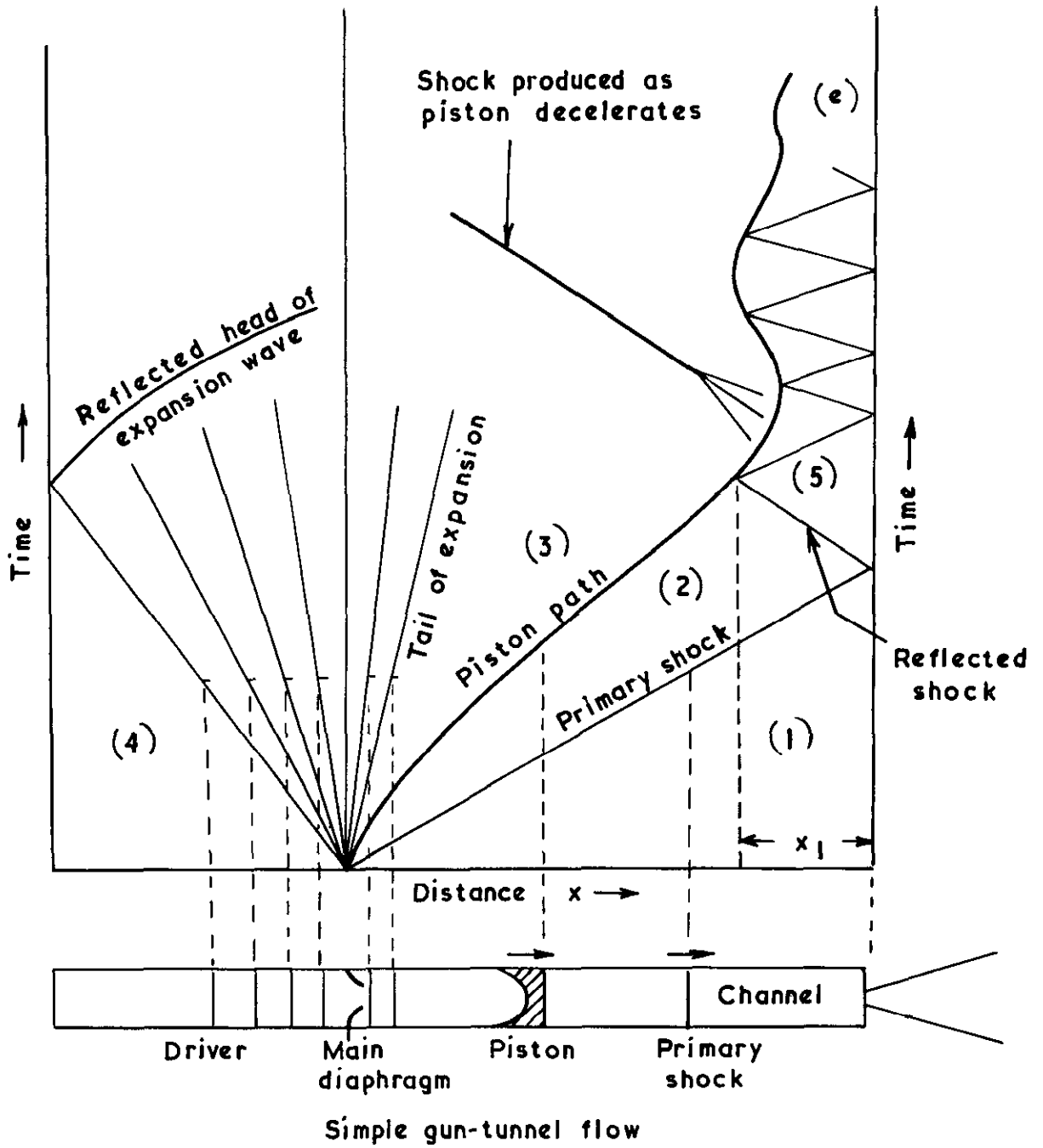
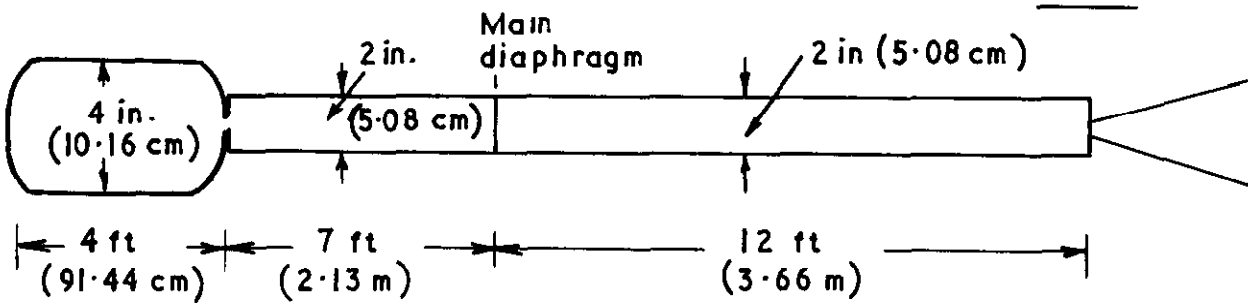
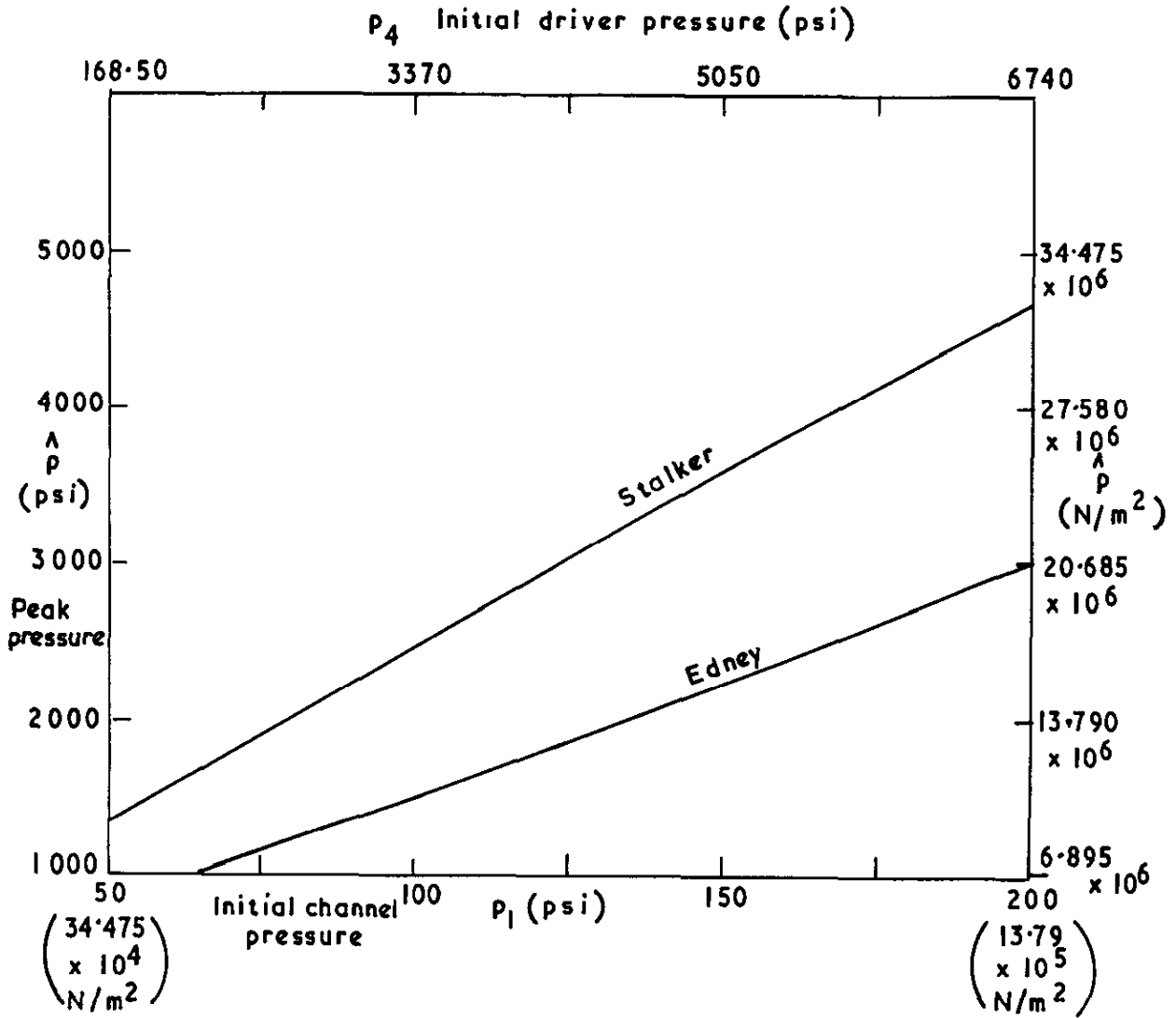


FIG 2



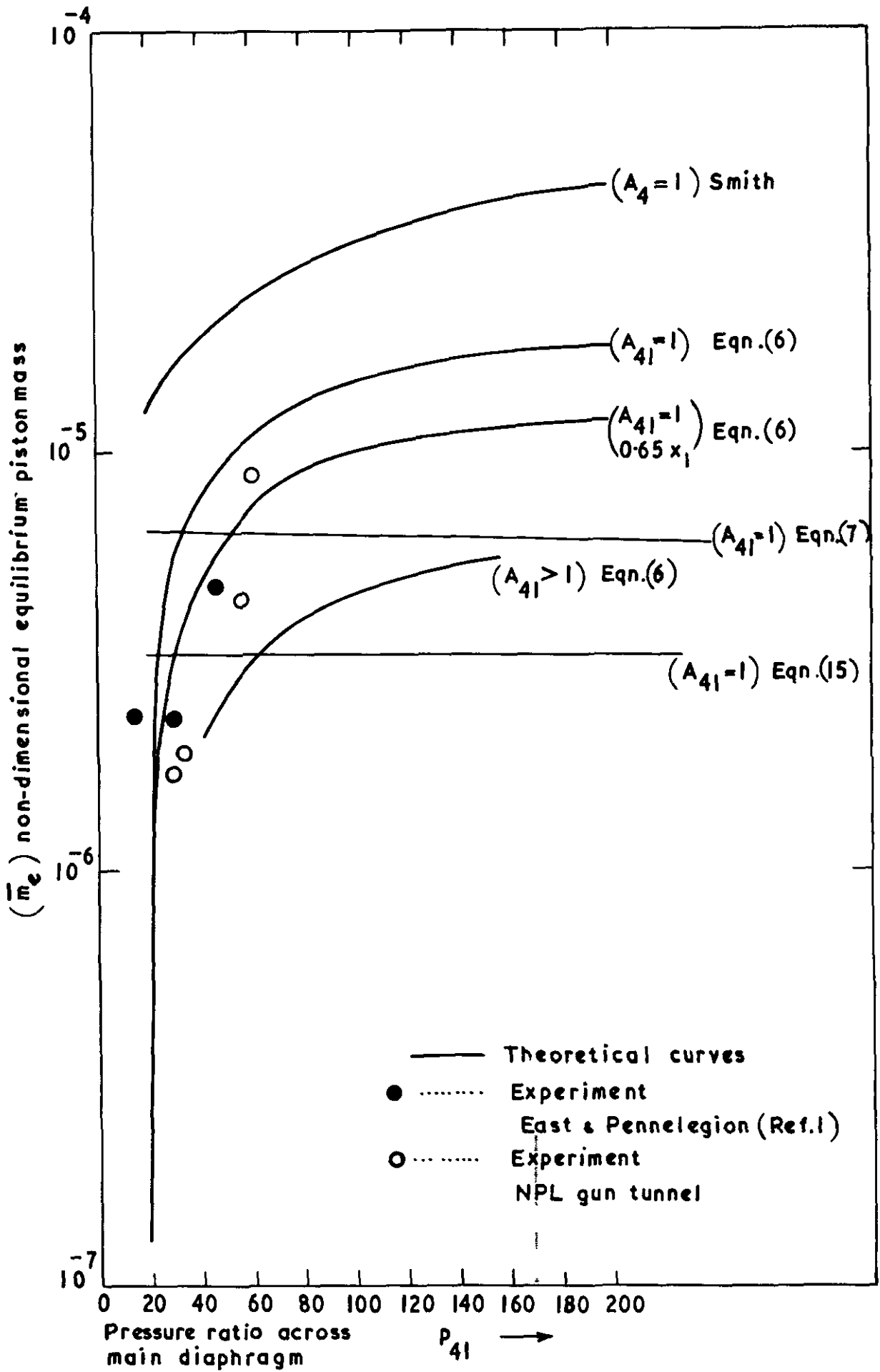
NPL 2 in. gun-tunnel dimensions.

FIG. 3

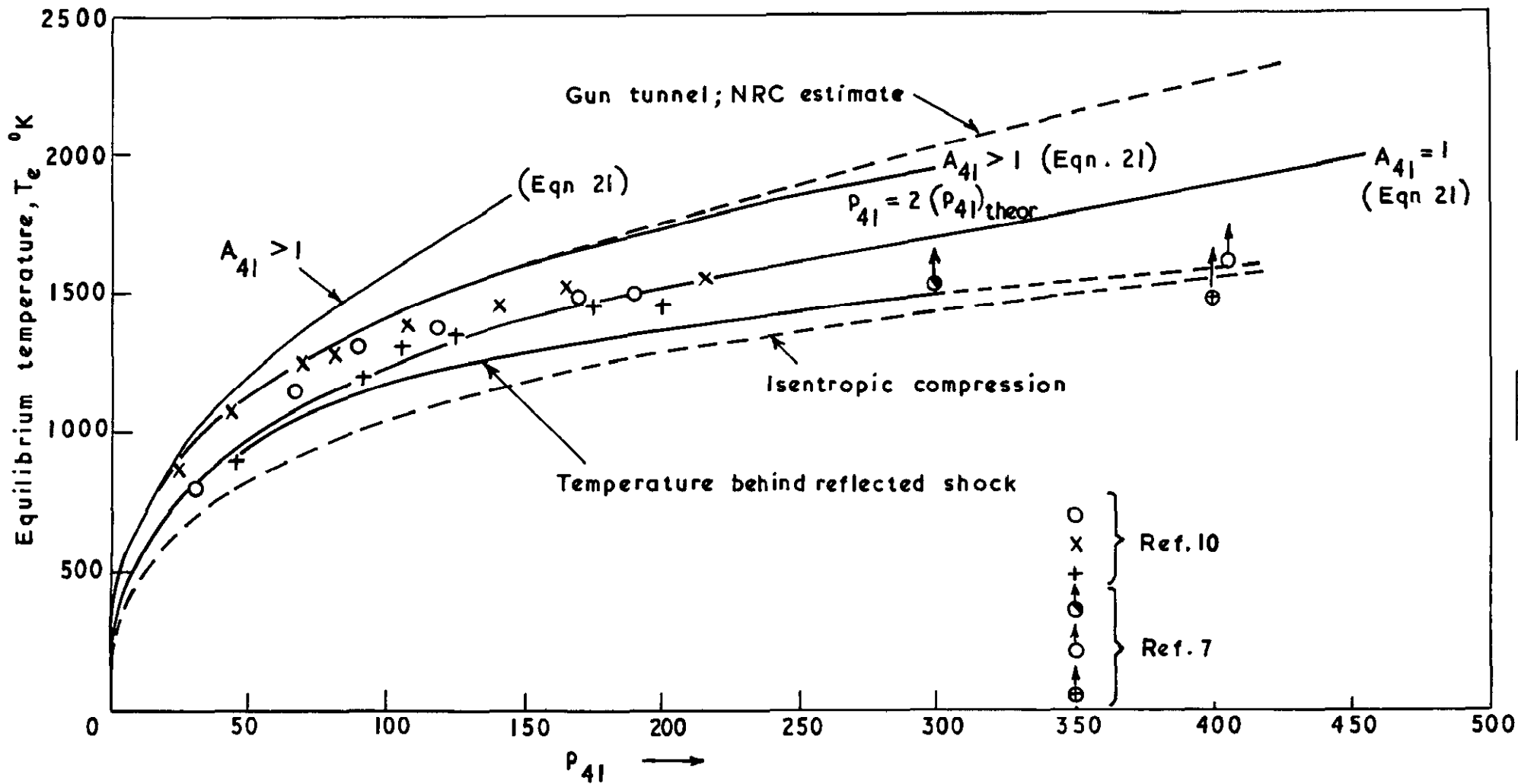


Peak pressure versus initial driver and channel pressures using Stalker's and Edney's formulae.

FIG. 4



Curves of \bar{m}_e vs. p_{41} using the various formulae.



Gun tunnel temperature measurements (Ref. 7) versus theory.

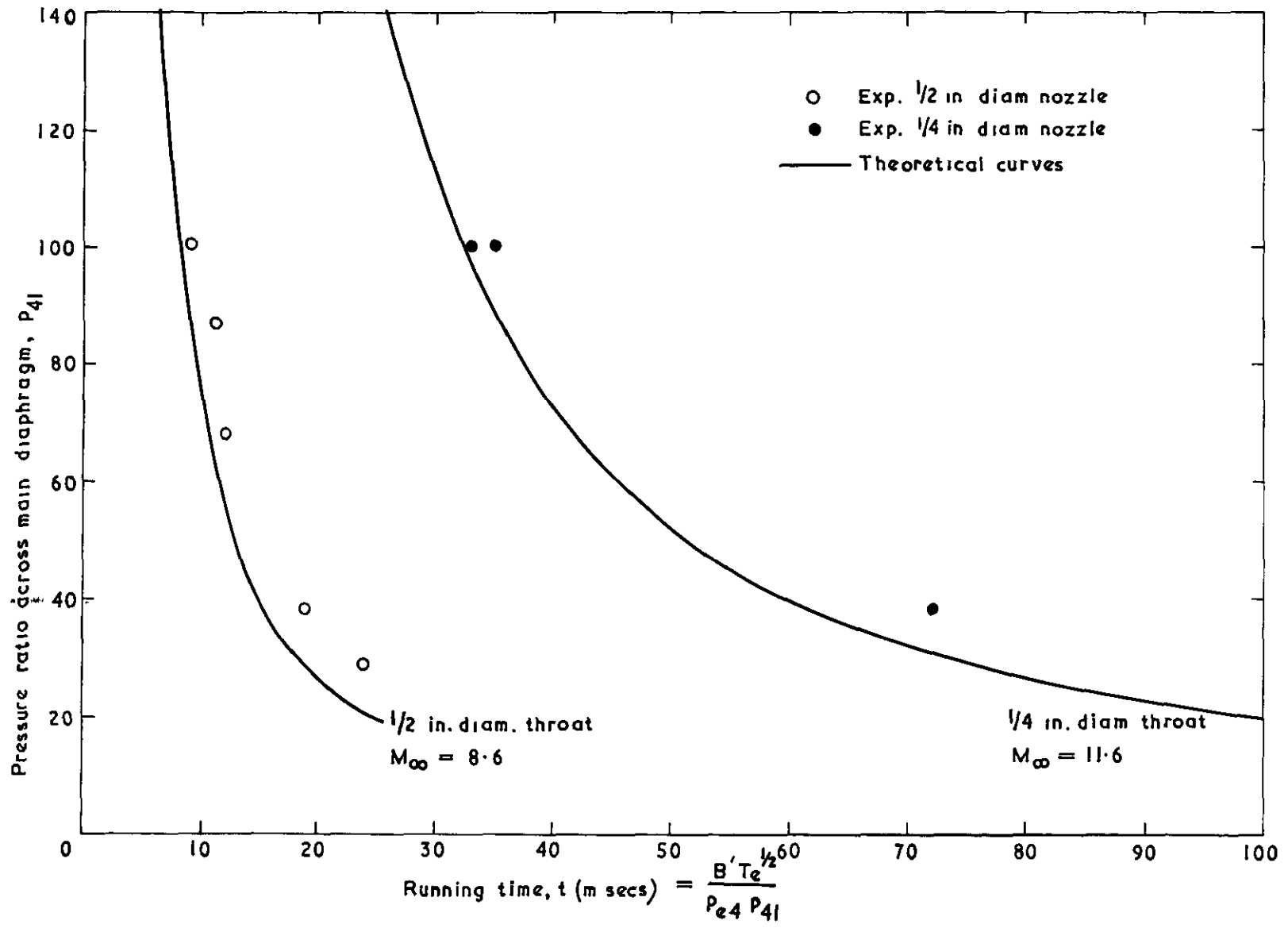
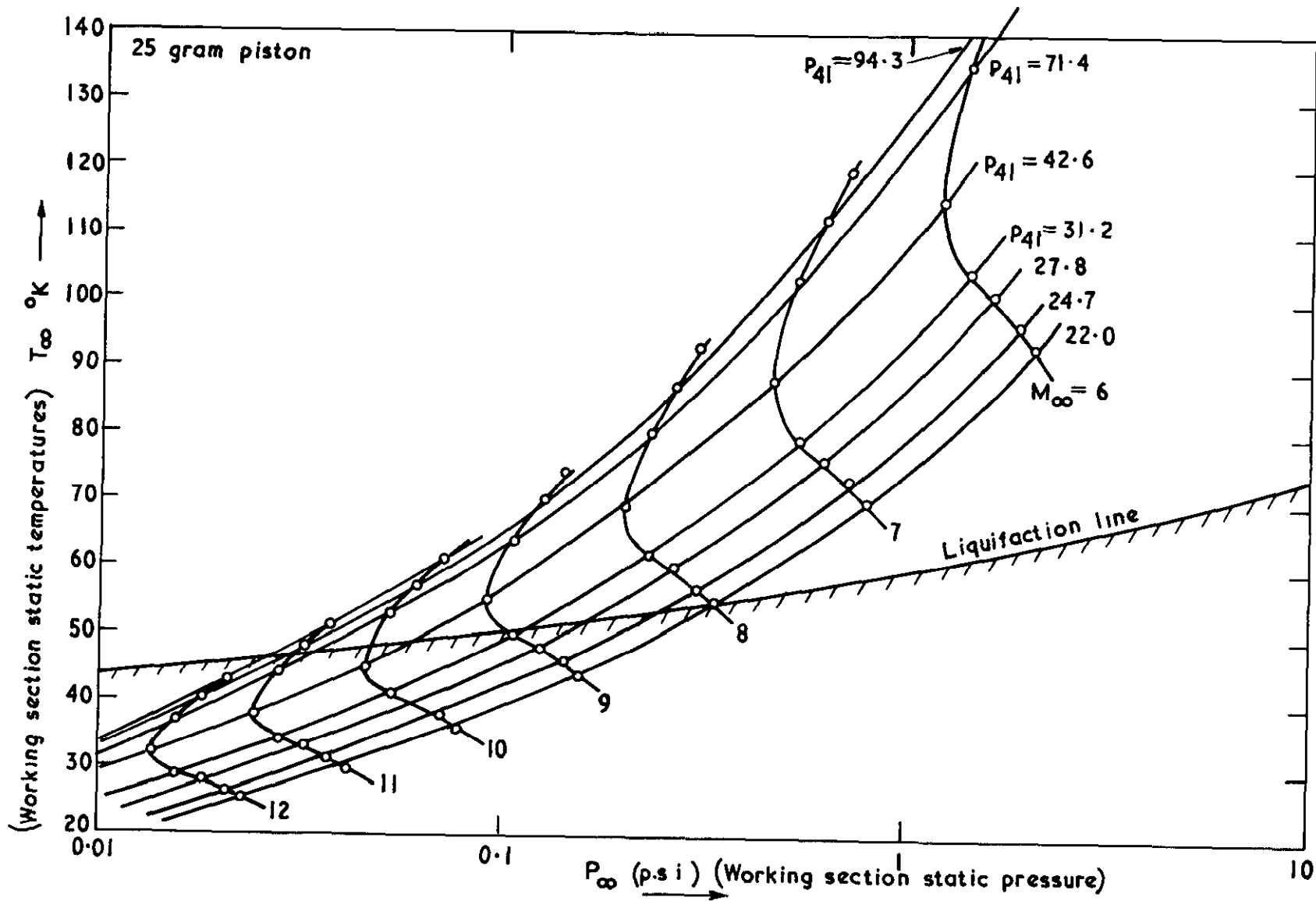


FIG. 6

Gun tunnel running time for various diaphragm pressure ratios



Working section static temperatures and pressures for various P_{41} and M_{∞}

25 gm. Piston

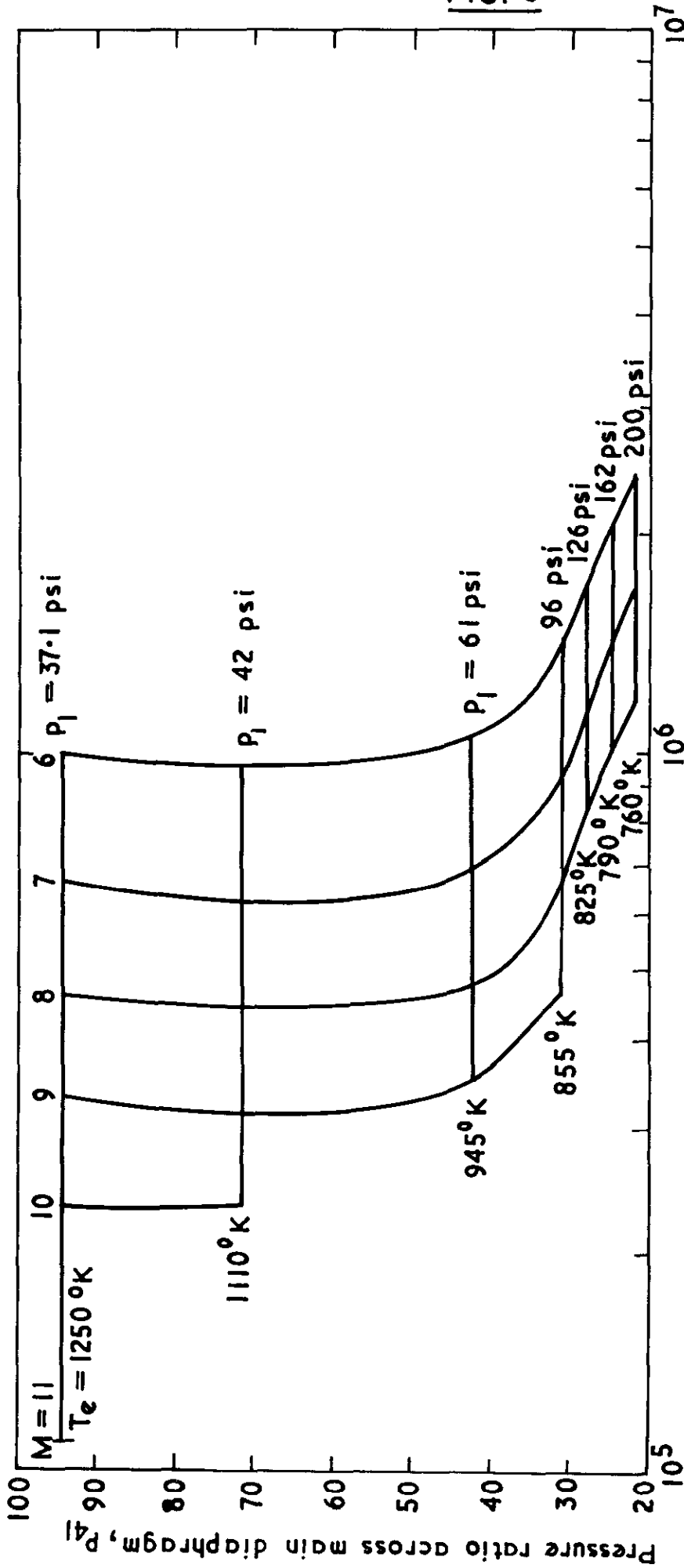
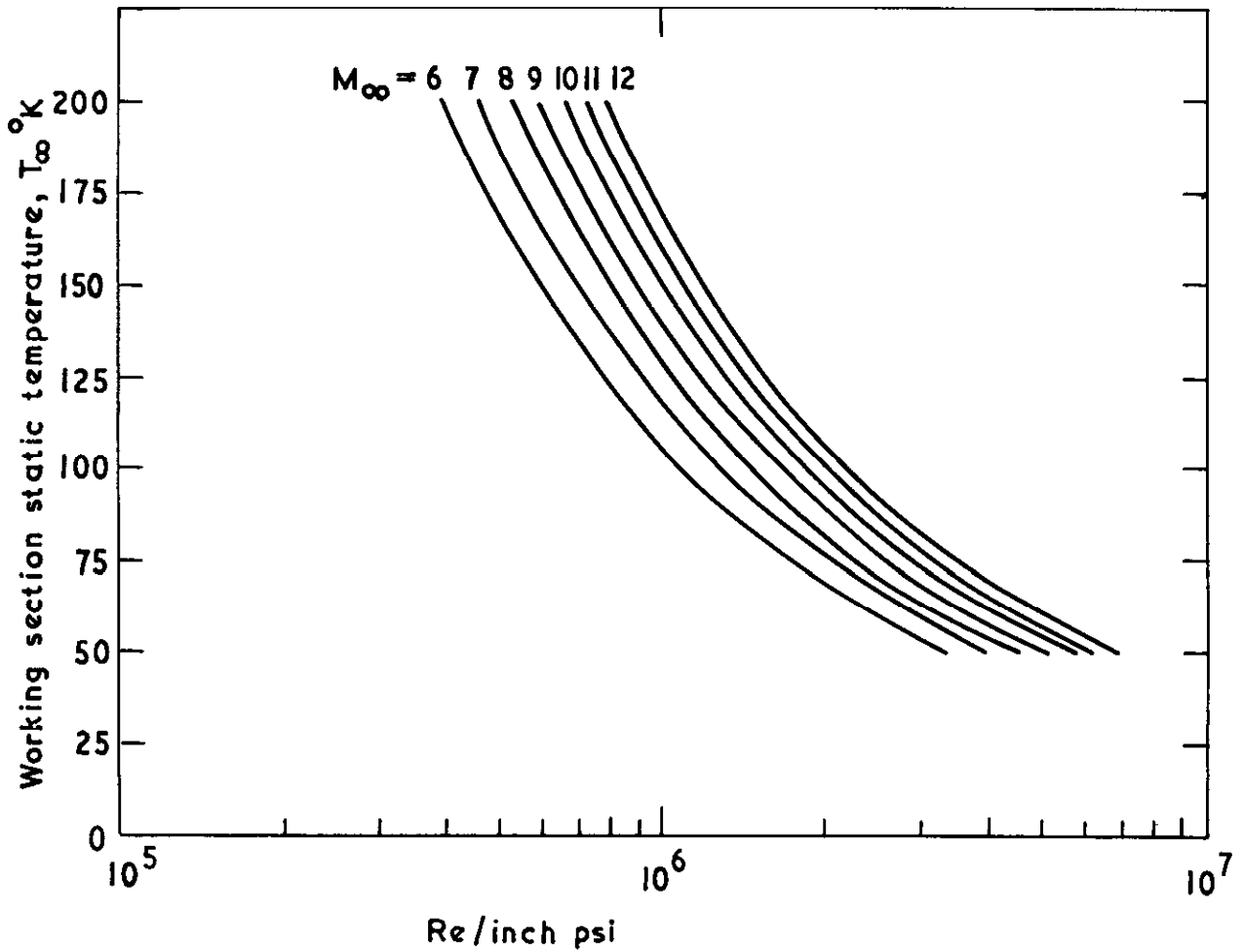


FIG. 8

Reynolds number per inch versus P_{41} and M_{∞}

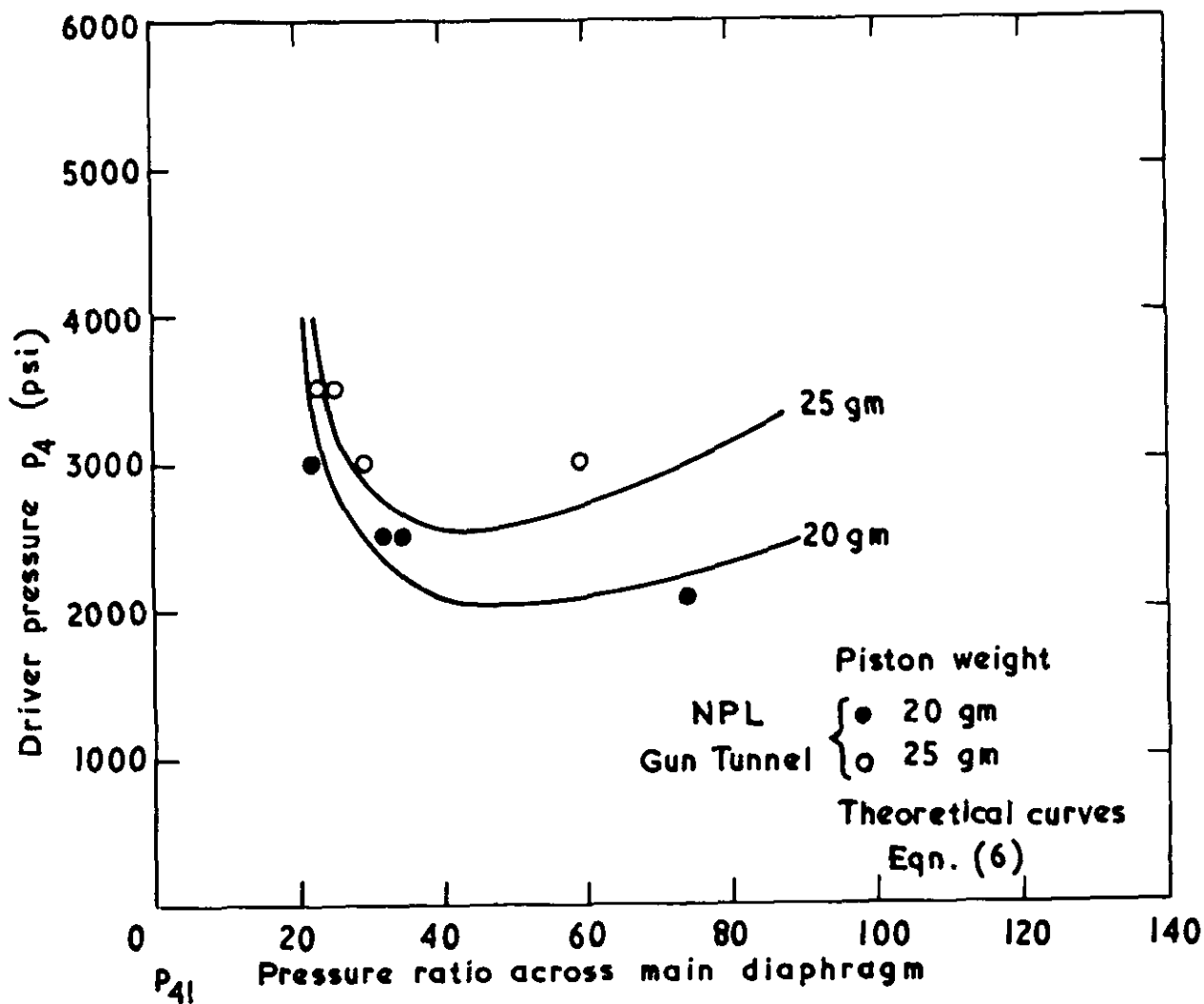
FIG. 9

$$\text{Re / inch psi} = \frac{8.4 \times 10^6 \times M_\infty (T_\infty + 117)}{T_\infty^2}$$



(Multiply by P_∞ for Re/inch)

FIG.10



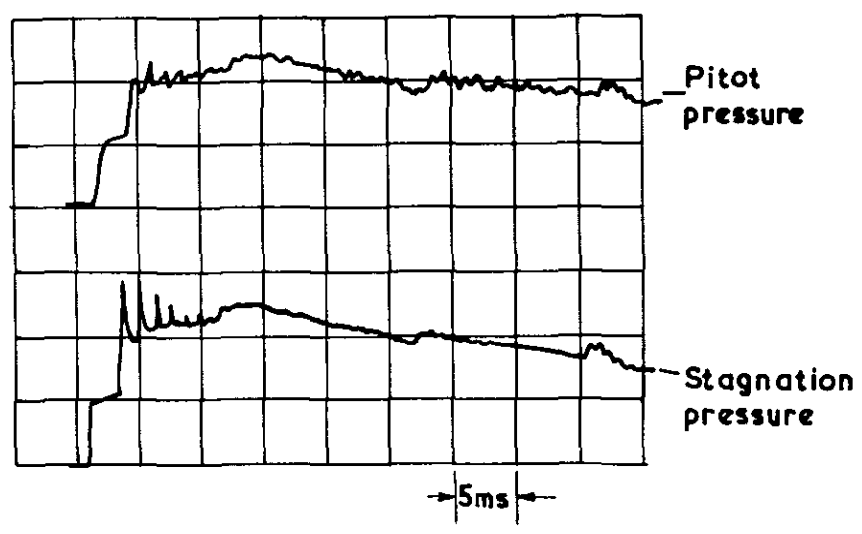
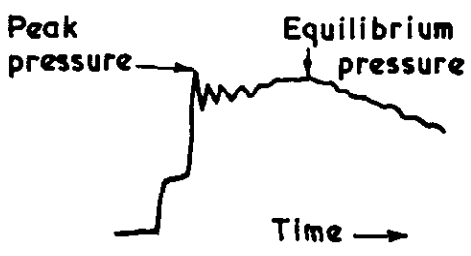
Variation of equilibrium piston mass with P_{41} and P_1

20 and 25 piston weights

FIG. 11(a&b)



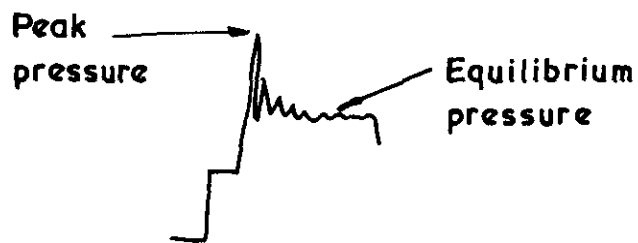
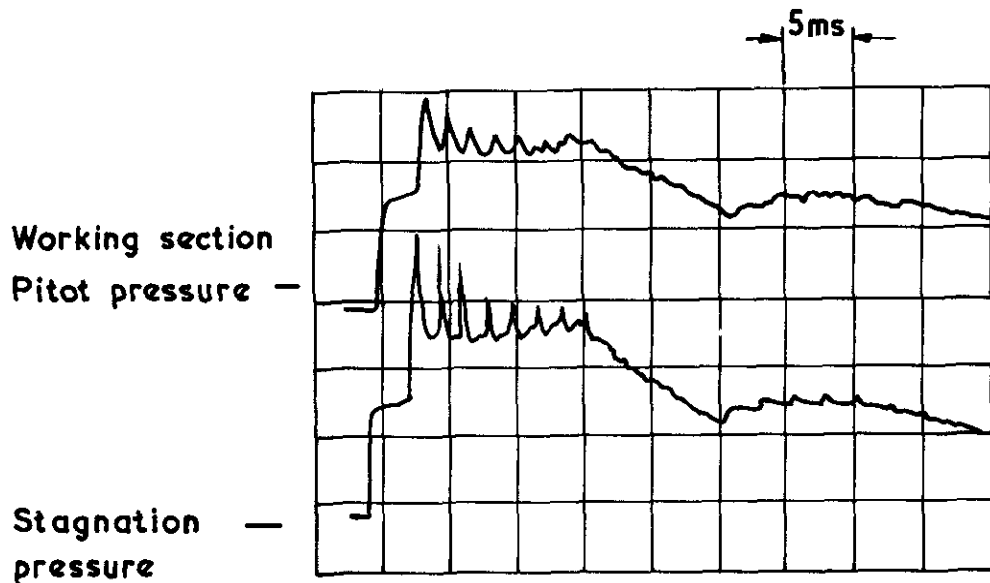
(a)
 $m_e = 20 \text{ gms}$
 $P_4 = 3000 \text{ psi}$
 $p_1 = 110 \text{ psi}$
Top trace pitot pressure
Bottom trace reservoir stagnation pressure



(b)
 $m_e = 25 \text{ gms}$
 $P_4 = 3000 \text{ psi}$
 $p_1 = 90 \text{ psi}$

Reservoir stagnation and working section pitot pressure traces
Working gas nitrogen

FIG. 11 (c)



This trace demonstrates the off design condition when a 20gm piston is used with $p_4 = 1000$ psi, $p_1 = 50$ psi.

The driver pressure is therefore below the minimum value for this piston weight, as seen in Fig. 10.

A.R.C. C.P. No. 982

July, 1967

Davies, L., Regan, J. D. and Dolman, K. A.

ON THE EQUILIBRIUM PISTON TECHNIQUE IN GUN TUNNELS

The use of the equilibrium piston technique in gun tunnels is discussed. Details of a simple theoretical formula for the calculation of ideal piston weight are given together with results of experiments performed in the NPL 2 in. gun tunnel using 20 to 25 gm pistons.

A.R.C. C.P. No. 982

July, 1967

Davies, L., Regan, J. D. and Dolman, K. A.

ON THE EQUILIBRIUM PISTON TECHNIQUE IN GUN TUNNELS

The use of the equilibrium piston technique in gun tunnels is discussed. Details of a simple theoretical formula for the calculation of ideal piston weight are given together with results of experiments performed in the NPL 2 in. gun tunnel using 20 to 25 gm pistons.

A.R.C. C.P. No. 982

July, 1967

Davies, L., Regan, J. D. and Dolman, K. A.

ON THE EQUILIBRIUM PISTON TECHNIQUE IN GUN TUNNELS

The use of the equilibrium piston technique in gun tunnels is discussed. Details of a simple theoretical formula for the calculation of ideal piston weight are given together with results of experiments performed in the NPL 2 in. gun tunnel using 20 and 25 gm pistons.

© *Crown copyright 1968*

Printed and published by

H I R M A J E S T Y ' S S T A I O N E R Y O F F I C E

To be purchased from

49 High Holborn, London WC 1

423 Oxford Street, London W 1

13A Castle Street, Edinburgh 2

109 St Mary Street, Cardiff CF1 1JW

Brazennose Street, Manchester 2

50 Fairfax Street, Bristol 1

258/259 Broad Street, Birmingham 1

7-11 Linenhall Street, Belfast BT2 8AY

or through any bookseller

Printed in England